International Journal of Signal Processing, Image Processing and Pattern Recognition
Vol. 8, No. 2 (2015), pp. 223-236
http://dx.doi.org/10.14257/ijsip.2015.8.2.21

A Remote Sensing Industrial Solid Waste Image Segmentation Method Based on Improved Watershed Algorithm

Wenxing Bao and Bing Yu

School of Computer Science and Engineering, Beifang University of Nationalities, Yinchuan Ningxia 750021, P. R. China
bwx71@163.com

Abstract

Taking the high-resolution remote sensing image of industrial waste dump as the research object, this paper proposes a new image segmentation method based on marker-controlled watershed transform and region merging. The method gets the finial partition result by two-phrase segmentation on the pan-sharpened true color ALOS image. In the first phase, color gradient image of original image should be calculated and then it is modified by morphological impose minima, which should use markers extracted in two different ways. Lastly, preliminary segmentation result is obtained by watershed transform operates on the modified color gradient image. To solve the over-segmentation of industrial solid waste and other ground objects, region merging operation is performed according to the similarity measure criterion based on segmented objects' color histogram Bhattacharyya coefficient in the second phrase, and then the final result is obtained. This method has been tested on the pan-sharpened ALOS image of 2.5 meters resolution in Shizuishan industrial zone, China. Experiment results demonstrate that this method is feasible and effective to segment the remote sensing industrial solid waste image.

Keywords: *industrial solid waste image, remote sensing image segmentation, watershed algorithm, region merging*

1. Introduction

With the rapid development of economy and industrialization, the produced and accumulated quantities of industrial solid wastes are increasing. However, such traditional means as ground monitoring can not meet the current needs of environment protection. It is because remote sensing owns the advantages such as large-scale monitoring, lower costs, space continuity and long-term monitoring that we could extract industrial solid waste disposal site, which is wide distribution and irregular, from remote sensing images. So in order to significantly reduce the difficulty of manual monitoring, we should find an effective extraction method based on the characteristics of industrial solid waste images.

Object-oriented classification is an efficient way to extract information from high-resolution remote sensing image. The method is not only using the object's spectrum, but also sufficiently using object's geometry information and structural information [1]. Since image analysis and processing are based on the object as the basic unit, so object observation is an important precondition for the object-oriented remote sensing industrial solid waste image processing. The objects are usually obtained by image segmentation. Image segmentation is the separation or consolidation operation of the pixels and then the objects in image processing could be obtained. Image object is the closed area, which is composed of several pixels. The segmented objects should be corresponding to the actual ground objects to some extent. The quality of segmentation algorithm directly affects the results of information extraction and terrain classification.

ISSN: 2005-4254 IJSIP

Currently, there are three types of image segmentation methods, segmentation based on threshold value, segmentation based on edge detecting and region-based segmentation. But in the actual application of image segmentation, segmentation method based on threshold value usually can not get better results for high-resolution remote sensing image which is with abundant details, and the drawback of segmentation with edge detecting is that it is difficult to solve the contradiction between noise immunity and detection precision. In contrast, region-based image segmentation could make full use of the various properties of remote sensing image [2], and it generally could get segmented regions which are with high homogeneity. And so it is, we use this method in this paper. Images with industrial solid wastes have characteristics such as irregularly distributed and different in size and prominence, so in view of these characteristics, this paper researches a new method which could segment the industrial solid waste images.

In 1991, Vincent and Soille [3] put forward the famous watershed algorithm based on immersion simulation. On the basis of this algorithm, this paper gives an improved method to make it fit for remote sensing industrial solid waste segmentation. Watershed transform gives image some one pixel width closed boundaries which would help the extraction of objects' information. In addition, this algorithm not only has relatively high efficiency and accuracy but also has advantage in stability and applicability. With the development of mathematical morphology, watershed segmentation has been broadly used in medical images, natural images and video images [4-6]. However, it also has flaws, which are more sensitive to noise and particularly easy to produce over-segmentation regions. Marker-controlled watershed algorithm [7] was proposed as well as verified that it could solve this problem well. But this method also has some weaknesses. Although domestic and foreign scholars put forward many methods to this approach, most need consider particular scope images. This paper brings this method into the segmentation of high-resolution remote sensing image which has complicated objects. And by analyzing the characteristics of industrial solid wastes in images, the paper provides a new way which combines marker-controlled watershed segmentation and region merging to solve this kind of image segmentation. Figure 1 shows the flowchart of the segmentation algorithm.

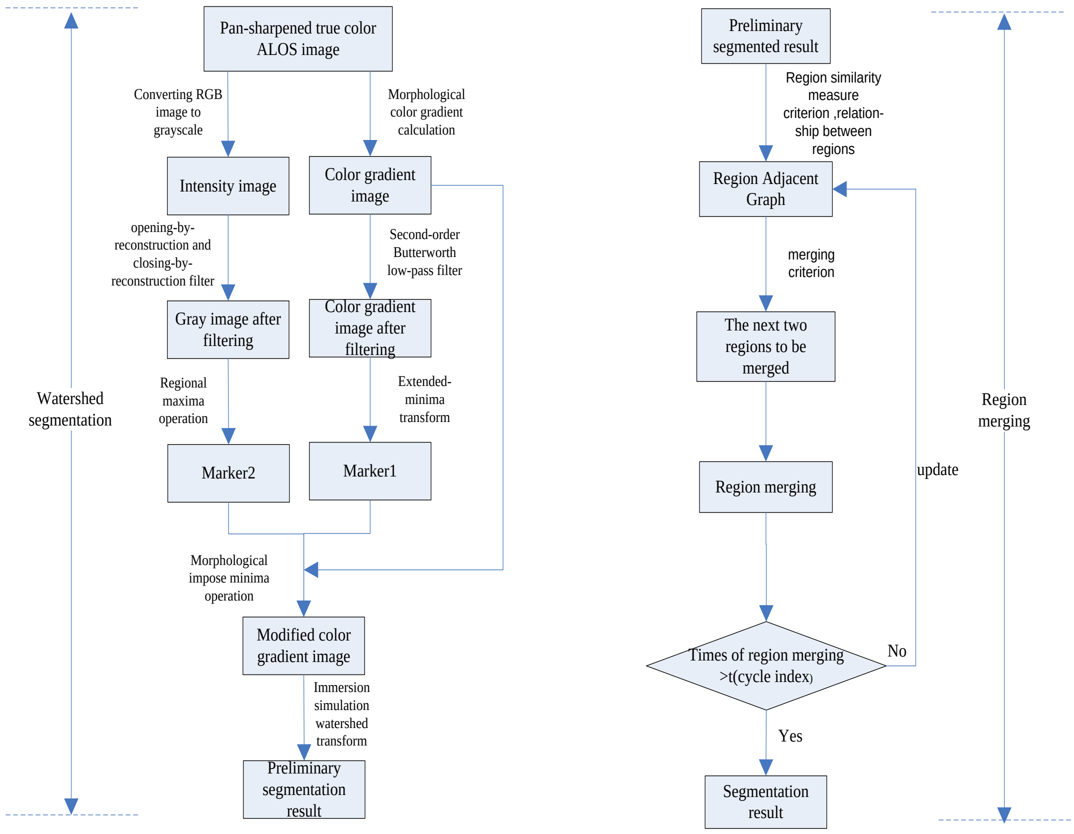

Figure 1. The Flowchart of the Segmentation Algorithm

2. Segmentation based on Marker-controlled Watershed and Region Merging

Marker extraction could greatly reduce bogus local minimum in gradient image before watershed transform, and thus reduce the number of over-segmentation regions at source. Then rapid region merging, which is on the basis of marker-controlled watershed segmentation, would obtain a better segmentation result. And so it is, the following region merging which consider region information is usually used to optimize segmentation results [8-9]. So we first segment image using watershed transform to get some regions which with high homogeneity and then do region merging in this paper. Thus the efficiency of this watershed algorithm would improve greatly while guarantee the accuracy.

2.1. Morphological Color Gradient Calculation

Gradient image could reflect the trend of changes better than original image. Practice shows that watershed algorithm has more connections with the gradient of image rather than the image itself [10]. So gradient image is more suitable to be the input image of watershed segmentation. Morphology gradient makes grayscale bounce input image more intense. Morphological gradient calculated by symmetrical structure element rely less on the direction of edge than the gradient calculated by spatial template. And morphological gradient is insensitive to noise. So this paper uses grayscale morphology gradient operator. Let I denote the original gray level image and each pixel (x,y) with gray level $I(x,y)$. Morphological gradient [11] can be represented by:

$$\nabla_B(I) = (I \oplus B) - (I \Theta B)$$
(1)

Where $\nabla(\cdot)$ is morphological gradient operation, $(I \oplus B)$ and $(I \Theta B)$ represent morphological image dilation and erosion respectively, B is a structure element and its shape is disk in this study.

To take advantage of the remote sensing images' spectral information, this paper uses true color image and the 3rd band, 2nd band and 1st band are used. Then, we use RGB color space to calculate the color gradient [11] and the definition is given by:

$$\nabla f = \vee\{\nabla_B(I_1), \nabla_B(I_2), \nabla_B(I_3)\}$$
(2)

Where ∇f is the morphological color gradient image of color image *f(x,y)*, $\nabla_B(I_1)$, $\nabla_B(I_2)$ and $\nabla_B(I_3)$ respectively represent the gradient image of three channels and it is calculated by formula (1). Symbol $\vee$ represents maximum, and it means that separately working out the gradient images of three components' corresponding primary color images and choosing the maximum pixel by pixel from the three gradient images. The obtained color gradient image could make original image's noise isolated and strengthened in certain degrees. This approach not only provides effective support to restrain noise but also converts the remote sensing image which is to be segmented into 256 gray-scale image.

2.2 Marker Extraction

2.2.1 Second-order Butterworth Low-pass Filter: Color gradient image without filtering processing is very sensitive to dark noise and texture detail. Direct mark minimum using original color gradient image would have lots of bogus minimum point which could lead over-segmentation. So smoothing filtering is required to eliminate interference minimum point. According to the illumination-reflectance model of image, we know that low-frequency components correspond to the main content of image and high-frequency components correspond to the edge, texture detail and noise of image. Low frequency components of image obtained by low-pass filter are the color gradient image's main content. Thus this paper adopts second-order Butterworth low-pass filter, it is the compromise between effective low-pass filter and acceptable ringing characteristics [12]. And Image ∇f^{BLPF} is filtering result which is obtained using second-order Butterworth low-pass filter to color gradient image ∇f .

2.2.2 Marker Extraction from Low-frequency of the Color Gradient Image: The method based on marker-controlled watershed is a better way to solve over-segmentation and the key is to find a set of makers or seed points corresponding to various objects of the image. This paper introduces the morphological marker method, which is extended-minima transform [13], to extract minimum marker from color gradient image, limiting the number of local minimum points and then getting the binary marker image. The extended-minima transform has two steps, the image is transformed by H-minima firstly, and then extracting regional minimum. It is given as follows:

$$\nabla f^{mark1} = E\min(\nabla f^{BLPF} \mid h)$$
(3)

Here ∇f^{BLPF} is the color gradient image obtained after second-order Butterworth low-pass filtering, and $E\min(\cdot)$ represents morphological extended-minima transform. Image ∇f^{mark1} is the binary marker image extracted from ∇f^{BLPF} . If the difference between minima's pixel value and its neighboring pixels' value is less than threshold *h*, the minima is eliminated. And if the different is greater than threshold *h*, the minima is marked. After extended-minima transform, each independent minima point either be eliminated or be extended to be larger and meaningful region. So color gradient image's minima region decline in the number and increase in the area. Threshold *h* is the key of marker extraction. Too small value of *h* could not make the extent to local minimum obviously and lead to over-segmentation. Too large value of *h* would often lose the real local minimum and lead to under-segmentation. It is usually a predetermined experience value. This paper uses the empirical method by experiments, and we can take the value around variance of all local minimum in image ∇f^{BLPF} .

2.2.3 Gray Morphological Reconstruction Filter: Reconstruction is a morphological transform which involves two images and one structure element. One image is maker, which is the start of transform. Another image is mask, which is used to restraint the process of transform. Structure element is used to give the connectivity. Let *I* as the mask and *J* as the maker, and $J \subseteq I$, reconstructing *I* from *J* can be expressed as $\gamma^{rec}(J, I)$, it could defined by the following iterative process. Firstly, h_1 is initialized to be the maker image *J*, structure element is created. Secondly, repeat the expression (4) until $h_{k+1} = h_k$. Lastly, h_{k+1} is the result, and $\oplus$ represents morphological dilation formula (4).

$$h_{k+1} = (h_k \oplus b) \bigcap I \tag{4}$$

The basic operations of mathematical morphology, such as erosion, dilation, opening and closing, all could remove the noise to some extent. Opening-by-reconstruction and closing-by-reconstruction are the commonly used method of morphological filtering. Image processing by them could well remove and weaken all kinds of noise which is less than the structure element in the bright regions and dark regions of image. And there are also some advantages of it compared to the image processing methods only using opening and closing operation. Such as unable changing the inner structure of original image, having little effect to the edge of image, having no edge movement, obtaining the main outlines of objects.

Gray-scale image filtering processing via opening-by-reconstruction and closing- by-reconstruction is defined as follows: the process of opening-by-reconstruction is that morphological erosion operation, which is using structure element *b*, should be applied to the original gray image firstly and then taking the result as the marker image and taking the original image as the mask image, executing the morphological reconstruction operation; it can be written as $I_{o\_rec} = \gamma^{rec}(I \Theta b, I)$ .And the closing-by-reconstruction should be the followed operation. Morphological dilation operation also should be applied to the original gray image and the result image is denoted by I_d . Taking the complementary set of I_d as the marker image and taking the complementary set of I_{o_rec} as the mask image, executing the morphological reconstruction operation. The result of this morphological reconstruction filtering is written by I_{oc_rec} .

2.2.4 Marker Extraction from Gray Image of the Original True Color Image: If the image is segmented using only ∇f^{mark1} participation in the marker-controlled watershed transform, we would find adhesions among different objects. The noise is effectively removed by the process above, but some objects' information would be lost. These objects, which are not separated, are not be marked as local minimum in the color gradient image before watershed transform. So it is unable to pinpoint the exact location of border and part of weak edges would be lost. By adjusting the value of threshold *h* in the operation of extended-minima transform, the phenomenon of adhesion could be solved in some degree, but a lot of meaningless over-segmentation regions would be produced. As the supplementary of marker ∇f^{mark1}, this method also extracts the additional marker from gray image of the original true color image based on gray morphological reconstruction filtering.

We get the regional maximum binary image from the result of morphological reconstruction filtering (I_{oc_rec}). And small modification operations of closing, erosion and opening would be applied to the regional maximum binary image. After these operations, the maker image I^{mark2} is obtained.

2.3 Watershed Transform

The original color gradient image is modified by morphological impose minima [13]. And regional minima of original image exist only when the corresponding binary maker image areas are nonzero. The modified gradient image is denoted by ∇f^{ws}.

$$\nabla f^{ws} = IM\min(\nabla f, \nabla f^{mark1} \cup I^{mark2})$$

(5)

Where $IM\min(\cdot)$ is impose minima operation, ∇f is original color gradient image, $\nabla f^{mark1} \cup I^{mark2}$ represents the union of the two markers.

$$f^{WS} = WTS(\nabla f^{ws})$$

(6)

The watershed regions of input image ∇f^{ws} are obtained by the operation of watershed transform, operation $WTS(\cdot)$ represents watershed transform and the result is f^{ws}.

2.4 Region Merging

Although the result objects obtained by the aforesaid watershed segmentation have good homogeneity, too much objects and the over-segmentation of solid waste stacking area exist in the field of remote sensing industrial solid waste images segmentation. To improve the efficiency and accuracy of industrial solid waste segmentation, this paper merges the regions on the basis of the result of watershed transform.

2.4.1 Region Similarity Measure Criterion: The key problems of region merging are the definition of merging criterion, the setting of merging order and the rule of merging termination. The definition of merging criterion is usually described by region similarity measure, and the value of it would often affect the order and frequency of region merging.

A region could be described in many features such as color, texture and shape. This paper introduces the color histogram [15] to represent the segmented objects and uses the value of it to describe the similarity measure criterion. It is because the feature is less affected by the segmentation algorithm compared with others. The colors of different segmented regions from the same ground object often have a high similarity. This paper uses RGB color space to compute the color histogram. Each color channel all should be quantized into 16 levels uniformly and the color histogram of each region should also be calculated in the feature space of $16\times16\times16=4096$ bins. Bhattacharyya coefficient is used to measure the similarity between the normalized histogram of one region and its adjacent regions. The Bhattacharyya coefficient ρ between region R and region Q is defined as follows:

$$\rho(R,Q) = \sum_{i=1}^{4096} \sqrt{Hist_R^i \cdot Hist_Q^i}$$

(7)

Where $Hist_R$ and $Hist_Q$ are the normalized histograms of region R and region Q, the superscript i represents the different bins of them. Bhattacharyya coefficient $\rho(R,Q)$ also is the region similarity measure criterion. The larger the Bhattacharyya coefficient is, the higher the similarity between R and Q is. The geometric explanation of $\rho(R,Q)$ is the cosine of the angle between the two vectors in Formula (8). The smaller the angle of two vectors is, the larger the cosine and the Bhattacharyya coefficient are：

$$\left(\sqrt{Hist_R^1},...,\sqrt{Hist_R^{4096}}\right)^T \; and \left(\sqrt{Hist_Q^1},...,\sqrt{Hist_Q^{4096}}\right)^T \tag{8}$$

The method is a simple and intuitive method to measure the similarity of adjacent regions. Color histogram is global description, so the method is less sensitive to the small change of local noise. Since Bhattacharyya coefficient is the inner product, it also makes the method have a strong anti-noise ability.

2.4.2 Region Merging Process: The RAG (Region Adjacent Graph) is used in the paper, and formula (9) gives the merging criterion which determines the next two regions that are needed to merge.

$$P(R_i, R_j) = \max_{i=1\cdots n,\, j=1\cdots n} \rho(R_i, R_j), i \neq j, R_i \; is \; adjacent \; to \; R_j \tag{9}$$

Here $P(R_i, R_j)$ represents the location of region R_i and region R_j in the region adjacent graph, $\rho(R_i, R_j)$ is the similarity coefficient of R_i and R_j. After region merging, the two regions become one region, *i.e.*, $R = R_i \cup R_j$. The steps of region merging are as follows:

(1) Counting the region adjacency relationship and building RAG: If R_i and R_j are adjacent, separately calculate the normalized histogram of each region and calculate the Bhattacharyya coefficient between R_i and R_j, storing the value into corresponding position in the RAG. If R_i and R_j are not adjacent, the value of similarity is zero.

(2) Region merging: Choosing the maximum similarity of the RAG and merging the corresponding two regions. Updating the RAG (the similarities between new region R and its adjacent regions are only needed to calculate).

(3) Merging termination: The merging termination is determined by the value of parameter t (cycle index).

3. Experiment and Analysis

3.1 Experiment Data and Environment

This paper takes the ALOS high-resolution remote sensing image as the test data, the imaging time is August 18, 2008. The resolution of images is 2.5m and size is 512×512. The fusion image is obtained by 10m multi-spectral image and 2.5m panchromatic image. It is the remote sensing image of Ningxia Shizuishan industrial area, China. The bands combination of the test true color image is band3, band2, and band1 and respectively corresponds to the channel of R, G, and B. The complexity of ground objects is higher by observation and artificial digital segmentation would take much time. So this paper implements the image segmentation of industrial solid wastes by programming. The experiment environment is Intel Core 2 CPU, 2.40 GHz personal computer and matlab2012a.

3.2 Experimental Procedures

The experimental procedures of this paper are as follows:

Step 1: Calculating the morphological color gradient of original true color image.

Step 2: Using second-order Butterworth low-pass filter to the color gradient image and then extracting the first maker image ∇f^{mark1} using the method in section 2.2.2.

Step 3: Using the gray-scale morphological reconstruction filter to the gray image of original true color Image and extracting the second marker image I^{mark2} using the method in section 2.2.4.

Step 4: Using morphological imposes minima method to modify the original color image and then preliminary results of segmentation are obtained.

Step 5: Using the region merging method in section 2.4 to merge the preliminary result objects and the final segmentation results are obtained.

Step 6: Doing quantitative analysis and qualitative analysis to final segmentation result.

3.3 Experimental Results

In order to verify the feasibility and effectiveness of the method, this section gives some experimental results. Figure 2(a) shows the original true color fusion ALOS image. The ground objects of Figure 2(a) are following: roofs, blue ceilings, cinder stacking areas, bare lands, roads, building gaps, lime piles, trees, etc. Cinder stacking areas and lime piles are all the industrial solid waste in Figure 2(a). We can see that the ground objects are complexity and there are no apparent bounds between industrial solid wastes and bare lands. For convenience, Figure 2(b) gives the reference image by manual segmentation (colored areas are the industrial solid waste regions).

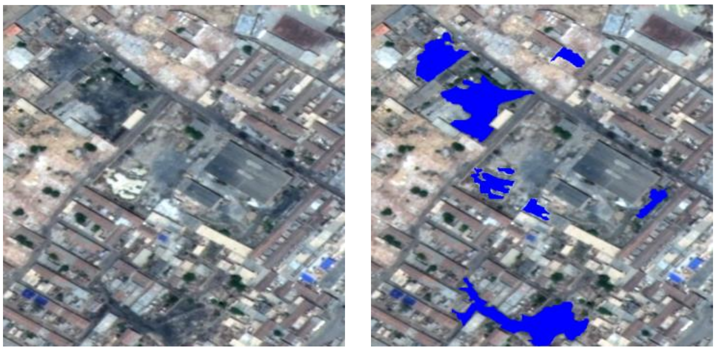

(a) (b)

Figure 2. (a) Original True Color Pan-sharpened ALOS Image, (b) Reference Industrial Solid Waste Image Regions by Manual Segmentation

To better understand the effect to the watershed segmentation results using different markers, Figure 3 gives the binary marker images of Figure 2(a), and figure 4 shows the corresponding segmentation results of Figure 2(a) using these three different makers. Figure 4(a) is the segmentation result which only uses the marker ∇f^{mark1}, we can see that the building gaps has adhesions with buildings, industrial solid wastes could not be separated with bare lands and building gaps, and some weak borders are lost. Figure 4(b) shows the result which only uses the marker I^{mark2} and the effect is also not good. Figure 4(c) is the final segmentation result which uses the marker $\nabla f^{mark1} \cup I^{mark2}$ and solves the problem in figure 4(a) well. Figure 5 more clearly shows the distinction among segmentation results which use different markers. In Figure 5, the abscissa means the one-dimensional coordinates of 500th line, ordinate means the corresponding intensity. Let ∇f^{ws1} denote the gradient image modified using the marker ∇f^{mark1}, ∇f^{ws12} denote the gradient image modified using the marker $\nabla f^{mark1} \cup I^{mark2}$. And note that, the number of minima regions in color gradient image after morphological impose minima operation corresponds to the number of objects in original image after watershed segmentation. So we can see that the extra minima regions in ∇f^{ws12} could supplement the gaps of minima regions in ∇f^{ws1}. Figure 5 commendably explains the reason of improvement from the result of Figure 4(a) to the result of Figure 4(c).

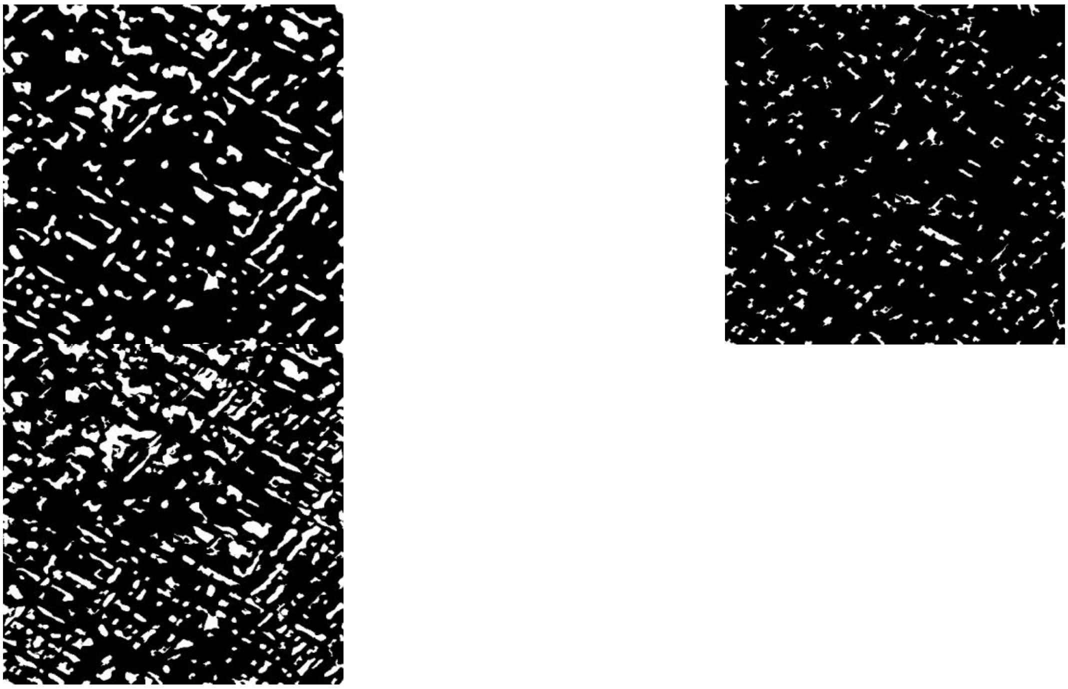

(a) (b) (c)

Figure 3. Marker Image: (a) Binary Image ∇f^{mark1}, (b) Binary Image I^{mark2}, (c) Binary Image $\nabla f^{mark1} \cup I^{mark2}$

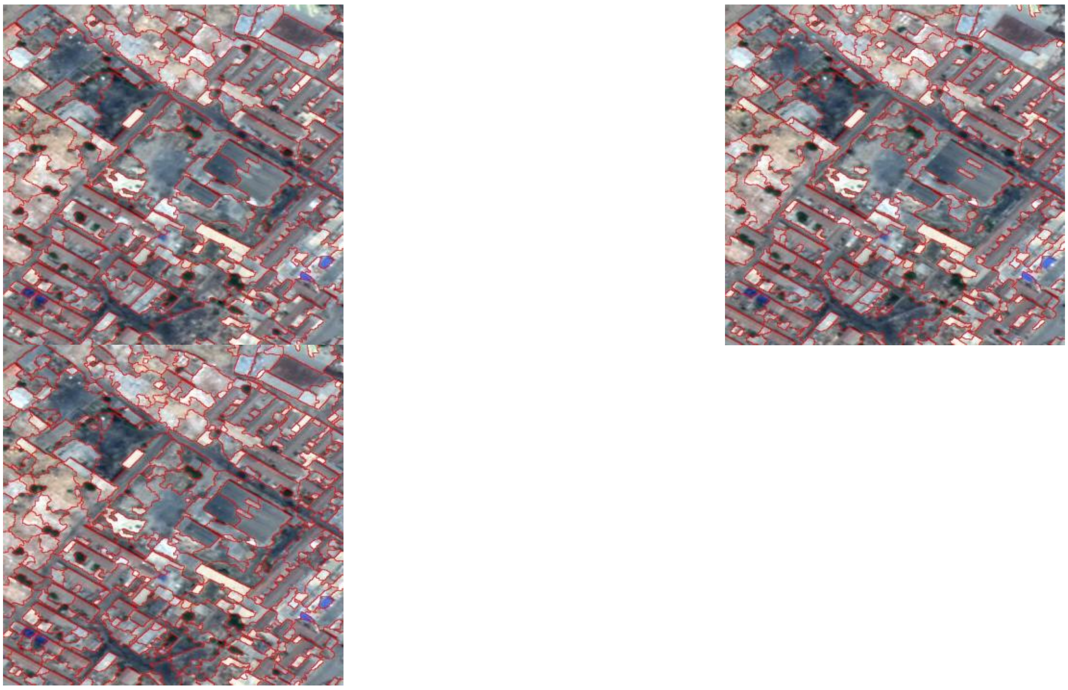

(a) (b) (c)

Figure 4. Preliminary Segmentation Result using Gradient Image Modified by Three Markers: (a) Modified by Marker ∇f^{mark1}, (b) Modified by Marker I^{mark2}, (c) Modified by Marker $\nabla f^{mark1} \cup I^{mark2}$

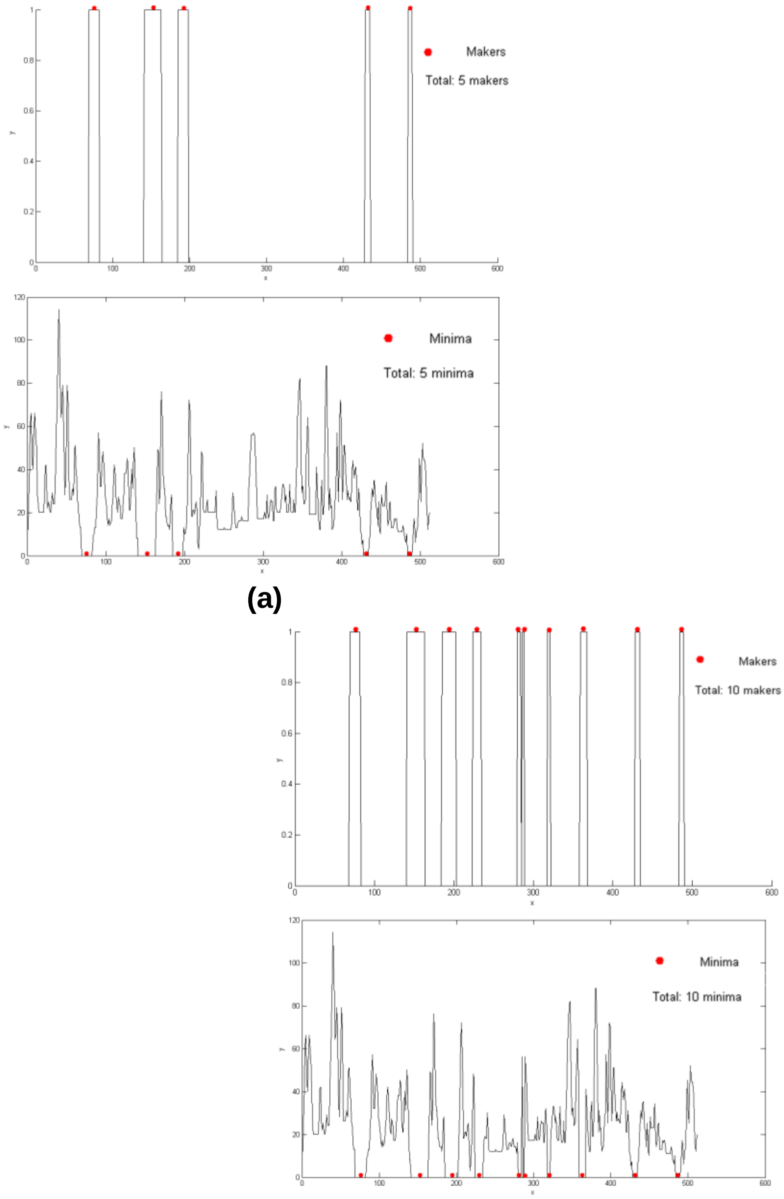

(a) (b)

(c) (d)

Figure 5. (a) The One-dimensional Intensity of Binary Image ∇f^{mark1} in Line 500, (b) the One-dimensional Intensity of Gradient Image ∇f^{ws1} in Line 500, (c) the One-dimensional Intensity of Binary Image $\nabla f^{mark1} \cup \nabla I^{mark2}$ in Line 500, (d) the One-dimensional Intensity of Gradient Image ∇f^{ws12} in Line 500

The final result segmented by the proposed method is compared with the result of EDSION segmentation and ENVI5.0 segmentation. The method of this paper has two needed parameters to adjust: *h* and *t*. To get a reasonable result using EDSION, reasonable selection of the parameters (*Spatial*, *Color*, and *Minimum Region*) is important. Feature Extraction, which is the oriented-object extraction tool of ENVI 5.0, has two segmentation steps: Over-segmentation and Merging. And the corresponding methods are Edge segmentation method and Full Lambda Schedule merging method, so there are two parameters to choose (*Scale* and *Merge*). The industrial solid waste areas are easily confused with the surrounding background, so the choice of parameters for the EDISON segmentation and ENVI5.0 segmentation are decided by repetition test, and the parameters used in the paper are more suitable for the segmentation of industrial solid waste. The contrast test results of the three segmentation algorithm are showed in Figure 6.

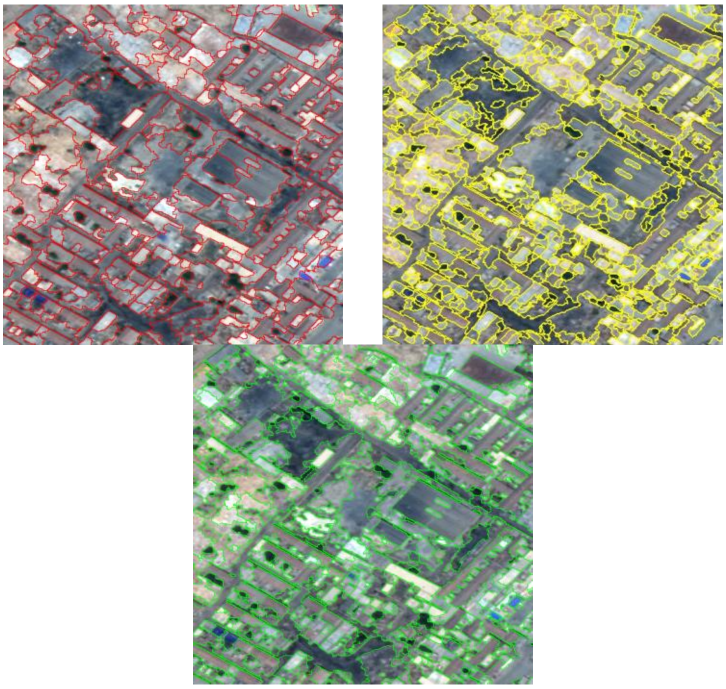

(a) (b) (c)

Figure 6. Segmentation Result: (a) Result using the Proposed Method (h=5, t=27), (b) Result using EDISON (Spatial=6, Color=5.8, Minimum Region=80), (c) Result using ENVI 5.0(Scale=30, Merge=95)

There is no uniform standard about image segmentation evaluation at present. This paper uses object-level consistency error (OCE) image segmentation metric method of multiple objects proposed by Polak [18] to measure the segmentation results of industrial solid waste. Let OCE meet $OCE(I_g, I_s) \in [0,1]$(I_g is the reference objects segmented by humans, I_s is the actual segmented objects). $OCE=0$ means that the segmented results are same with the reference segmented results, the smaller the value of OCE is, the better the segmentation result is. Figure 7 gives the three segmented results of industrial solid wastes (the colored regions). Table 1 gives the OCE values of the three methods.

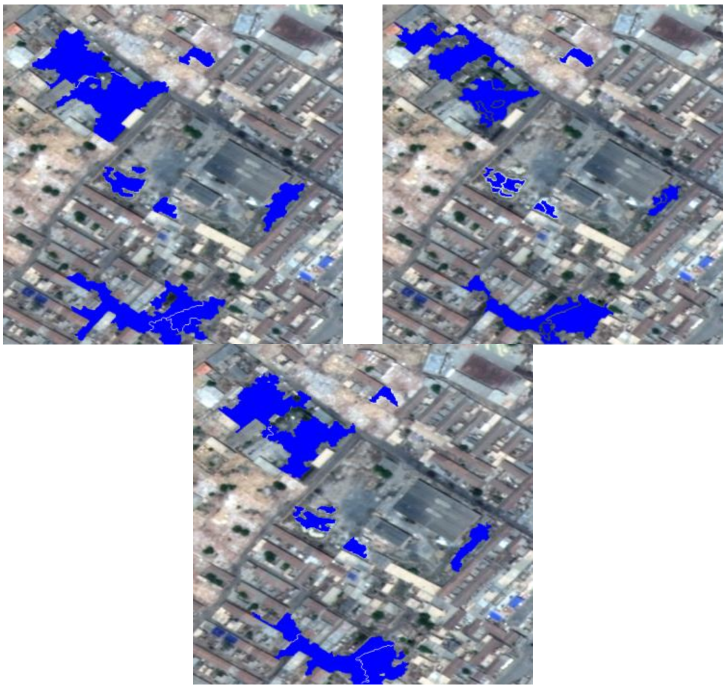

(a) (b) (c)

Figure 7. Segmented Industrial Solid Waste Regions: (a) the proposed method, (b) EDISON, (c) ENVI 5.0

Table 1. The Result Parameters Contrast of Different Methods

Method	Number of regions	OCE(solid waste regions)	Running times
Proposed method	343	0.0228	7.2s
EDISON	644	0.0567	2.6s
ENVI 5.0	755	0.0241	About 5.6s

3.4 Results Analysis

By analyzing these results in Figure 6, and Table 1, it can be concluded that this remote sensing industrial solid waste segmentation method has the following advantages: (1) the results of EDISON and ENVI 5.0 have over-segmentation and there are many meaningless regions. The total segmentation regions using the proposed methods are significantly less than the other two methods and the segmented objects are mostly corresponds to the actual areas or ground objects. This would provide convenient conditions for the object-oriented information extraction and reduce the difficulty of terrain classification (2). The OCE of the proposed method is less than the OCE values of ENVI 5.0 and EDSION, so this would provide accuracy guarantee for the extraction industrial solid waste. And by observation, the result using this algorithm could also separate the bare lands and roofs from solid wastes (3). The basic parameters (*h*, *t*) are relatively stable, and it would take little time on the adjustment of parameters. Taken together, the proposed method is an automatic and efficient method and it does not need much manual intervention. It has certain advantages in the segmentation of industrial solid wastes, which are wide distribution and irregular, compared with the ENVI 5.0 and EDSION.

4. Conclusion

In this paper, the proposed remote sensing industrial solid waste segmentation method gets the finial partition result by two steps, marker-controlled watershed transform and region merging. It is a simple and effective method. We have achieved the expected goal, and the effectiveness of segmentation also has been proved by comparative experiments, but this method also has some aspects which need to improve. First, although it partly could reduce human intervention, the final image segmentation result can not be obtained in self-correcting ways. Second, the time-consuming of the method is determined by the number of times to merge regions. So the following research work is needed to solve these problems.

Acknowledgements

This work is supported by National Natural Science Foundation of China (61162013, 61461003).

References

[1]. P. F. Xiao, X. Z. Feng and S. H. Zhao, "Segmentation of High-resolution Remotely Sensed Imagery Based on Phase Congruency", Acta Geodaetica et Cartographica Sinica, vol. 36, no. 2, **(2009)**, pp. 146-151.
[2]. B. Zhang and B. B. He, "Multi-scale Segmentation of High-resolution Remote Sensing Image Based on Improved Watershed Transformation", Journal of geo-information science, vol. 16, no. 1, **(2014)**, pp.142-150.
[3]. L. Vincent and P. Soille, "Watersheds in digital spaces an efficient algorithm on immersion simulations", IEEE Transaction on Pattern Analysis and Machine Intelligence, vol. 13, no. 6, **(1991)**, pp. 583-596.
[4]. J. Wu, Y. H. Zhang, J. Bai, W. L. Weng, Y. Wu, Y. Han and J. H. Li, "Tongue contour image extraction using a watershed transform and an active contour model", J T singhua univ(Sci &Tech), vol. 48, no. 6, **(2008)**, pp. 1040-1043.
[5]. X. P. Wang, C. Y. Hao and Y. Y. Fan, "Watershed Segmentation Based on Morphological Scale-Space and Gradient Modification", Journal of Electronics& Information Technology, vol. 28, no. 3, **(2006)**, pp. 485-489.
[6]. G. B. Yang, Z. Y. Zhang and S. F. Yu, "Automatic video object extraction algorithm based on wavelet and watershed", Journal on Communications, vol. 26, no. 3, **(2005)**, pp. 7-13.
[7]. P. Salembier and M. Pardas, "Hierarchical morphological segmentation for image sequence coding", IEEE Transaction on Image Processing, vol. 3, no. 5, **(1994)**, pp. 639-651.
[8]. L. Patino, "Fuzzy relations applied to minimize over segmentation in watershed algorithm", Pattern Recognition Letters, vol. 25, no. 6 **(2005)**, pp. 819-828.
[9]. S. Q. Liu and G. J. Zhang, "Fast region merging algorithm for watershed transform based on adjacency list", Journal of Beijing University of Aeronautics and Astronautics, vol. 34, no. 11, **(2008)**, pp. 1327-1330.
[10]. R. C. Gonzalez and R. E. Woods, "Digital Image Processing (Third Edition)", Prentice Hall, New Jersey, **(2010)**.
[11]. R. H. Jr, C.F.Flores and J.Barrera, "Color image gradients for morphological segmentation", IEEE Proceeding of SIBGRAPT 2000, Gramado, Brazil, **(2000)**, pp. 316-322.
[12]. L. Gao, S. Y. Yang and H. Q. Li, "New Unsupervised Image Segmentation via Marker-Based Watershed", Journal of Image and Graphics, vol. 12, no. 6, **(2008)**, pp. 1025-1032.
[13]. P. Soille, "Morphological Image Analysis Principles and Applications (Second Edition)", Springer-Verlag, Berlin, **(2008)**.
[14]. X. Zhang and W. B. Chen, "A cell Edge Detection Algorithm Based on Morphological Reconstruction and Multi-structure", Computer Simulation, vol. 26, no. 8, **(2009)**, pp. 216-219.
[15]. J. F. Ning, L. Zhang, D. Zhang and C. K. Wu, "Interactive image segmentation by maximal similarity based region merging", Pattern Recognition, vol. 43, no. 2, **(2010)**, pp. 445-456.
[16]. D. Comanicu and P. Meer, "Mean Shift: A robust approach toward feature space analysis", IEEE Trans. Pattern Anal, Machine Intell. , vol. 24, no. 5, **(2002)**, pp. 603-619.
[17]. ENVI 5.0 help. Exelis Visual Information Solutions, Inc. **(2012)**.
[18]. M. Polak, H. Zhang and M. H. Pi, "An evaluation metric for image segmentation of multiple objects", Image and Vision Computing, vol. 27, **(2009)**, pp. 1223-1227.

Authors

Wenxing Bao Received his Ph.D degree from Xi'An Jiaotong University, China, in 2006. He is a full professor in the School of Computer Science and Engineering of Beifang University of Nationalities, China. His research interests include remote sensing image processing, AI, computer vision, and computer graphics. He has published about 30 papers in international/national journals.

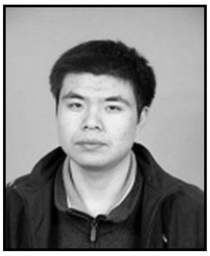

Bing Yu Received his B. S. degree in computer science and technology from Zhengzhou University, China, in 2011. Now he is working for his M.E. degree in School of Computer Science and Engineering of Beifang University of Nationalities, China. His research interests concentrate on digital image processing.